Co-published by
Institute of Fluid-Flow Machinery
Polish Academy of Sciences
Committee on Thermodynamics and Combustion
Polish Academy of Sciences

http://www.imp.gda.pl/archives-of-thermodynamics/

ARCHIVES OF THERMODYNAMICS

Machine Learning Optimisation of CI Engine Characteristics with WSA Algorithm and Prosopis Juliflora Biofuel

Sethuraman Narayanan, Vinodraj Subramanian, Thamizhvel Rajkumar, Vaithianathan Nadarajan

IFET College of Engineering, IFET Nagar, Gangarampalayam Post, Valavanur Villupuram 605108, Tamil Nadu, India
*Corresponding author email: mailmesethu@gmail.com

Received: 17.09.2025; revised: 03.11.2025; accepted: 16.11.2025

Abstract

Machine learning, a division of artificial intelligence (AI), empowers systems to gain knowledge from information and refine their capabilities over time. It uses algorithms to identify patterns and make prophecies or decisions. Prosopis juliflora is becoming gradually notorious as an optimistic substitute in biofuel inquiry. The mixing of Prosopis juliflora with diesel for use in combustion engines has been the subject of growing study in recent years. However, limited research has explored the impact of Prosopis juliflora on the compression ignition (CI) engine exhaust employing data-driven optimisation highlighting the need for new inquiries to address this shortfall. We aim to explore the cutting-edge and proficient machine learning driven weighted superposition attraction algorithm to optimise the efficiency and exhaust of CI engines powered with Prosopis juliflora biodiesel – diesel blends. Regression modelling is employed to define the relationships between factors such as the blend percentage and brake mean effective pressure (bar), and responses like the brake thermal efficiency (%), brake specific fuel consumption (g/kWh), smoke opacity (%), NO_x (g/kWh), CO (g/kWh), and HC (g/kWh). The data-driven weighted superposition attraction algorithm is subsequently employed to determine the best factor levels. Validation of the results demonstrates that the brake thermal efficiency is enhanced, while the other response variables are effectively reduced, showcasing the effectiveness of this methodology.

Keywords: Neural network; Machine learning; Juliflora; CI engine

Vol. 46(2025), No. 4, 117–125; doi: 10.24425/ather.2025.156842

Cite this manuscript as: Narayanan, S., Subramanian, V., Rajkumar, T., & Nadarajan, V. (2025). Machine Learning Optimisation of CI Engine Characteristics with WSA Algorithm and Prosopis Juliflora Biofuel. *Archives of Thermodynamics*, 46(4), 117−125.

1. Introduction

The scientific community is intensifying investigations into sustainable fuel technologies, responding to mounting environmental challenges and the critical imperative of reducing anthropogenic greenhouse gas contributions [1]. Emerging biofuel studies are utilising complex mathematical modelling and optimisation techniques – specifically Taguchi methods, genetic algorithm, response surface methodology (RSM), and integrated algorithmic frameworks like RF-NSGA III-TOPSIS – to systematically investigate and optimise combustion efficiency, engine performance, and emission characteristics [2]. Prosopis juliflora-based diesel biofuel represents a compelling technological solution, demonstrating remarkable capabilities in addressing critical environmental challenges through reduced greenhouse gas generation, enhanced air quality and decreased fossil fuel consumption [3]. The complex challenges of oil market volatility are catalysing transformative approaches to energy production, with Prosopis juliflora biomass-derived biofuels representing a technologically sophisticated strategy for reducing reliance on traditional fossil fuel resources [4]. Prosopis juliflora is produced from the seed of the Prosopis juliflora tree, commonly

Nomenclature

$d_{ij}(t)$– the i^{th} solution movement direction in the j^{th} dimension
$sl(t)$– step size
$x_{ij}(t)$– value for the i^{th} solution in the j^{th} dimension
X – feature
Y – outcome variable

Greek symbols
β – coefficient
ε – residual error term

Abbrevation and Acronyms
BMEP– brake mean effective pressure
BTE – brake thermal efficiency
CI – compression ignition
HC – hydrocarbon
NO_x – nitrogen oxides
RSM – response surface methodology
WSA – weighted superposition attraction

known as mesquite. The improved energy efficiency of engines powered by Prosopis juliflora mineral diesel renewable fuel has drawn significant interest from the freight industry, which is striving to reduce fuel usage and cut operating costs [5].

Prosopis juliflora mineral diesel renewable fuel holds significant potential as a sustainable energy solution for the future. Its properties closely align with those of standard diesel, making it a viable substitute for fossil fuels. Additionally, its ability to function seamlessly in mineral diesel or compression ignition (CI) engines excluding major adjustments has further fuelled research into its application [6]. These benefits support the position of Prosopis juliflora diesel biofuel as a promising alternative for complying with increasingly strict vehicle emission regulations. Several studies have shown that biofuel delivers a power output comparable to traditional diesel. The strong compatibility of Prosopis juliflora with diesel fuel provides a prospect to formulate a refined diesel – Prosopis juliflora blend with characteristics akin to pure diesel while effectively resolving phase separation issues [7]. Researchers have utilised both experimental methods and numerical simulations to probe the application of Prosopis juliflora in CI engines. The research examines the performance and emission traits of Prosopis juliflora biodiesel in diesel engines, emphasising key insights. The B25 blend demonstrated the most favourable results, offering thermal efficiency comparable to diesel while reducing emissions. Higher biodiesel percentages led to increased CO, HC and smoke emissions, but NO_x emissions dropped by 17.71%. Biodiesel was produced via transesterification using methanol and alkaline catalysts, showcasing its potential as an eco-friendly fuel alternative. The research identified B20 and B25 blends as optimal for achieving a balance between engine performance and emission control [8]. Additionally, an experimental study investigated the impact of adding diethyl ether (DEE) to Prosopis juliflora biodiesel blends on engine efficiency and pollutants. While the brake thermal efficiency (BTE) of biodiesel mixtures was slightly lower than that of pure diesel oil, the addition of DEE improved combustion efficiency. For instance, the B20DEE10 blend (20% biodiesel with 10% DEE) achieved BTE of 31.4% at 50% load compared to diesel's 36.7%. Moreover, the DEE additives reduced emissions such as CO_2, HC and CO, along with a decrease in NO_x emissions, attributed to DEE's elevated cetane grade and heat of vaporisation [9]. The investigation examines the efficiency of juliflora oil biodiesel in a compression ignition engine, showing a 5−7% increase in BTE and a 15–20% cutback in CO and HC exhausts compared to diesel. NO_x emissions were slightly higher by 10–12%, a common trade-off with biodiesel. Overall, the findings highlight juliflora biodiesel's potential for cleaner energy, with further optimisation needed for emission control [10].

This comprehensive research explores the adaptation of juliflora biodiesel and its variants as clean fuels in CI engines through a combination of simulation and experimental approaches. Studies demonstrate that juliflora biodiesel offers comparable engine performance with reduced emissions, establishing its viability as a sustainable fuel option [11]. Further investigation into H_2 boosting with Prosopis juliflora biofuel highlights performance and emission improvements using modern optimisation practices like RSM and artificial neural networks (ANN) [12]. Additionally, research on Prosopis juliflora methyl ester emphasises the role of transesterification in enhancing fuel properties, such as viscosity, to improve engine compatibility and efficiency [13]. Machine learning in engine research applies artificial intelligence (AI) practices to analyse data and past experiences in the domain of biofuels and engines. Through the application of algorithms and computational frameworks, it examines experimental or simulated data concerning engine efficiency, exhaust characteristics and Prosopis juliflora fuel properties. This methodology uncovers trends, enables forecasting and provides critical insights, aiding researchers in activities like determining ideal biofuel mixtures, forecasting engine behaviour and refining butanol production techniques. The rising significance of data-driven ANN has noticeably enhanced forecasting and optimisation initiatives. Extensive investigations have been conducted on biofuel applications in CI engines. Recent efforts have particularly examined the potential of Prosopis juliflora in diesel engines, leveraging machine learning techniques to determine optimal outcomes.

This research applies regression modelling for quantitative analysis and utilises the weighted superposition attraction (WSA) for optimising multiple objectives. The WSA technique is used to identify the optimal concentrations of Prosopis juliflora (vol. %) and brake mean effective pressure (BMEP) (bar) for multiple performance factors, such as BTE (%), brake specific fuel consumption (BSFC) (g/kWh), NO_x (g/kWh), HC (g/kWh), CO (g/kWh) and smoke opacity (%). The concurrent optimisation of these parameters using WSA is an innovative feature of this research, which seeks to integrate the WSA approach into biofuel studies within the context of CI engines.

2. Juliflora performance optimisation

The experimental approach described provides a structured method for studying how Prosopis juliflora biofuel blends perform in a diesel engine. The study involves adjusting the fuel

blend and engine settings, and using cutting edge techniques like the weighted sum approach to analyse the results. The experimental setup and process are shown in Fig. 1.

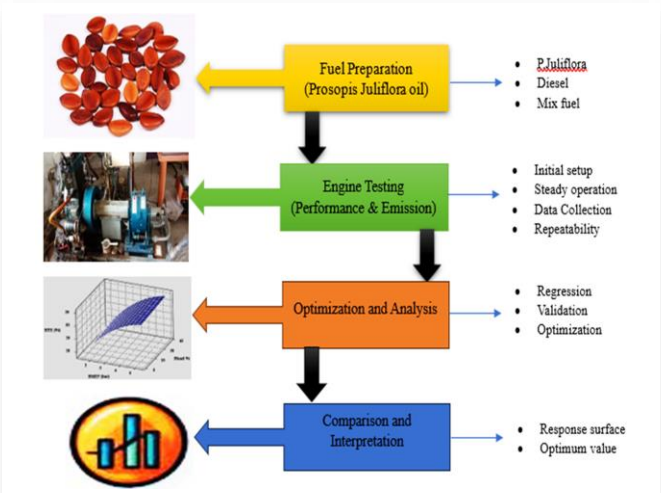

Fig. 1. Experimental methodology.

The study used different blends of Prosopis juliflora biofuel mixed with diesel as the trial fuels. The distinct proportions and readiness techniques for these blends are outlined in earlier research. Typically, the biofuels are made by combining pure Prosopis juliflora with conventional diesel at varying levels. The blends tested in the study include pure diesel, JB10 (10% Prosopis juliflora, 90% diesel), JB20 (20% juliflora, 80% diesel), JB30 (30% juliflora, 70% diesel), and JB40 (40% juliflora, 60% diesel), with their properties summarised in Table 1.

Table 1. Properties of mineral diesel and biofuel.

Features	Juliflora oil	JB10	JB20	JB30	JB40	Diesel
Density (g/cm³)	0.811	0.872	0.876	0.879	0.846	0.830
Kinematic viscosity (mm²/s)	3.707	3.963	4.019	4.515	3.819	43.96
Cetane number	61.97	59.72	54.15	50.21	59.10	46 - 55
Sulphur content (mg/kg)	59.344	58.11	84.30	111.79	65.93	6800
Higher heating value	36.763	39,457	39.60	39.94	38.279	42,500
Oxidation stability (110°C)	12.661	15.84	16.630	6.75	11.198	–
Oxygen content	8.6	8.4	12.2	14.02	10.49	–

Each fuel blend was carefully mixed and tested to ensure uniformity before being utilised in the trials. Subsequently, various operational conditions were applied to assess the engine's performance with each fuel blend. The key stages of the evaluation process are as follows:

(a) Primary setup.

The engine was heated to ensure consistent working temperatures throughout all the tests, and reference measurements were obtained using conventional diesel fuel to set a benchmark for comparison.

(b) Stable working conditions.

The engine was evaluated under different stable working conditions by adjusting BMEP. Typically, tests were performed at several load points, including 1.35, 2.70, 4.8 and 5.8 bar.

(c) Gathering data.

Essential engine metrics like BSFC, BTE and exhaust emissions were measured, alongside burning factors such as the heat release rate and in-cylinder pressure using sensors.

(d) Consistency and validation.

Each trial was conducted multiple times to confirm reliable and precise data.

The trial data were evaluated to determine the effects of various Prosopis juliflora diesel mixtures on engine efficiency and exhausts. The WSA approach was enforced to optimise the blends, granting the detection of the most potent mixture for elevating fuel efficiency and minimising emissions. Factors such as fuel blend ratio, engine load and speed were considered in the optimisation procedure. The results for the Prosopis juliflora blends were compared to the reference diesel fuel characteristics. The inquiry centred on detecting patterns in efficiency and exhausts, assessing the burning characteristics of Prosopis juliflora blends, and exploring the potential of Prosopis juliflora as a clean alternative to diesel fuel.

2.1. Test setup

The tests were carried out using a mono-cylinder CI engine, with the configurations and setup provided in Fig. 2.

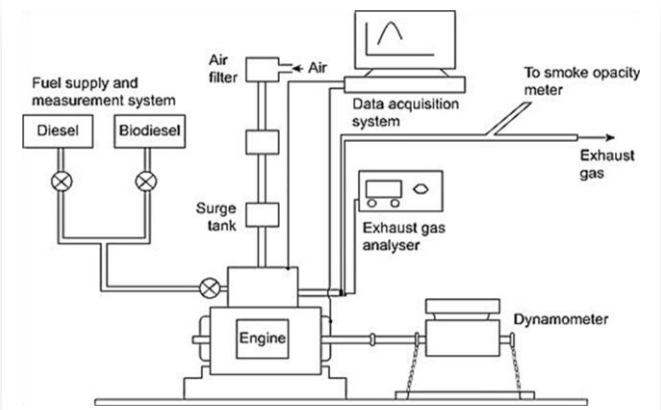

Fig. 2. Diesel engine setup.

2.2. WSA approach

The WSA algorithm is a modern optimisation method rooted in the broader field of metaheuristic algorithms and multi-objective optimisation. It extends the traditional weighted sum approach, which consolidates several objectives into one scalar value through a process of weighted summation. The emergence of WSA was driven by the increasing complexity of engineering problems, particularly in fields like energy systems, material sciences and automotive research, where advanced optimisation tools were needed. Recent developments have refined WSA to improve its efficiency and adaptability, making it suitable for

high-dimensional datasets and complex applications. In engine research, WSA has been applied to optimise multiple parameters, such as performance metrics and emissions, addressing the dual challenge of enhancing efficiency while meeting environmental standards. Its ability to balance multiple objectives simultaneously has made WSA a valuable tool for solving real-world problems, with its adoption steadily growing in engineering and environmental studies. The WSA algorithm directs the keys at repetition t near their designated search paths using the equation:

$$x_{ij}(t+1) = x_{ij}(t) + sl(t) \cdot d_{ij}(t) \cdot \left\| x_{ij}(t) \right\|. \quad (1)$$

In the WSA algorithm, $x_{ij}(t)$ represents the value of the j^{th} dimension for the i^{th} solution, while $sl(t)$ denotes the step size. The solution's movement direction is defined by $d_{ij}(t) \in \{1, 0, -1\}$ for dimension j. The term $\|x_{ij}(t)\|$ indicates the distance between the origin and the j^{th} dimension of solution i at the t^{th} iteration. The algorithm updates the solution along its dimensions in the specified search directions using the second term, $sl(t) \cdot d_{ij}(t) \cdot \|x_{ij}(t)\|$ as indicated on the opposite side of Eq. (1) [16].

3. Outcomes and analysis: diesel engine operated with juliflora biofuel and machine learning

Twenty experimental trials were carried out according to the experimental design. The findings from these trials are illustrated in Fig. 3 and Fig. 4. Regression models were created for uncoded factor levels, utilising the outcomes such as NO_x (g/kWh), Smoke Opacity (%), CO (g/kWh), HC (g/kWh), BSFC (g/kWh) and BTE (%).

The graphs in Fig. 3 illustrate the performance of diesel (D100) and biodiesel blends (JB10, JB20, JB30, JB40) in terms of BTE (%) and BSFC (g/kWh) as functions of BMEP (bar).

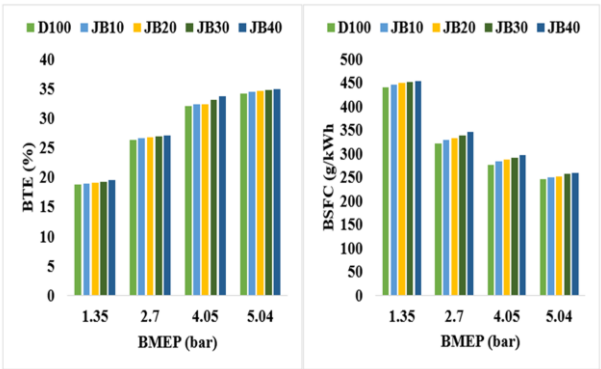

Fig. 3. History of BTE (%) and BSFC (g/kWh) vs. BMEP (bar).

BTE increases with BMEP for all fuels, peaking at approximately 38% at 5.04 bar. D100 consistently exhibits the highest BTE, while higher biodiesel blends show slightly reduced efficiency due to their lower calorific value and higher viscosity. At 1.35 bar, BTE ranges from 15–17%, with JB40 showing the most significant drop. By 4.05 bar, BTE rises to 30–33%, with JB10 and JB20 performing closest to D100, indicating that lower biodiesel blends maintain efficiency while incorporating renewable fuel. Conversely, BSFC decreases with increasing BMEP, from ~ 450–470 g/kWh at 1.35 bar to ~ 200–220 g/kWh at 5.04 bar. D100 achieves the lowest BSFC, reflecting its superior fuel efficiency. Biodiesel blends, particularly JB30 and JB40, show higher BSFC due to biodiesel's minimal energy density and elevated viscosity, which can affect combustion. However, JB10 and JB20 closely match the BSFC of D100, demonstrating a favourable balance between efficiency and renewable fuel use. Improved in-cylinder conditions at higher BMEP reduce the performance gap between diesel and biodiesel blends, making JB10 and JB20 optimal choices for maintaining efficiency while integrating biodiesel.

The graphs in Fig. 4 illustrate the emission characteristics of diesel fuel (D100) and biodiesel blends (JB10, JB20, JB30, JB40) across various brake mean effective pressures (BMEP).

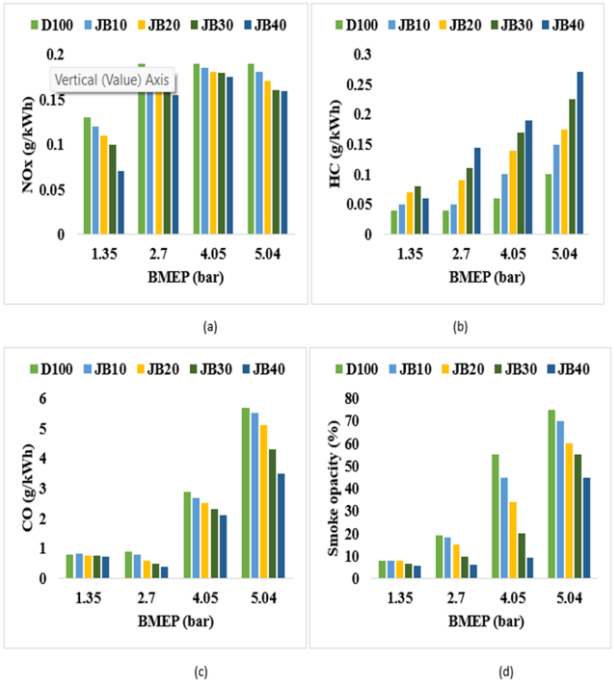

Fig. 4. History of Exhaust of (a) NO_x, (b) HC, (c) CO, and (d) Smoke opacity vs. BMEP (bar).

NO_x emissions increase steadily with BMEP for all fuels, peaking at 0.18–0.2 g/kWh at 5.04 bar. Biodiesel blends, particularly JB30 and JB40, exhibit higher NO_x emissions than D100 owing to their higher oxygen presence, which improves combustion but raises in-cylinder temperatures, promoting NO_x formation. At low load (1.35 bar), NO_x exhausts range from 0.05–0.1 g/kWh, with D100 showing the lowest levels due to the absence of oxygen and lower combustion temperatures. Hydrocarbon (HC) emissions are lowest at 1.35 bar, with biodiesel blends emitting less than D100, reflecting better combustion. At 2.7 bar, emissions increase slightly, with JB40 reaching about 0.1 g/kWh. At higher loads (4.05 and 5.04 bar), HC emissions rise significantly, peaking at 0.3 g/kWh for JB40 due to poor atomisation and reduced volatility in higher biodiesel blends. JB10 and JB20 demonstrate lower HC emissions, indicating bet-

ter combustion efficiency. Carbon monoxide (CO) emissions remain minimal at 1.35 and 2.7 bar, staying below 1 g/kWh for all blends, showing efficient combustion at low loads. At 4.05 bar, CO emissions increase, with JB40 emitting approximately 3 g/kWh. At 5.04 bar, CO emissions peak, with JB40 reaching 5.5 g/kWh, highlighting incomplete combustion and lower oxidation efficiency. D100 and JB10 perform better, keeping CO emissions below 5 g/kWh. Smoke opacity is minimal at 1.35 bar (<10%) for all fuels, indicating clean combustion. It increases slightly at 2.7 bar, with JB40 reaching 15%. At 4.05 bar, opacity rises significantly, with JB30 and JB40 reaching ~45%. At 5.04 bar, smoke opacity peaks at 70% for JB40 owing to elevated viscosity and inferior atomisation, which hinder burning. D100 consistently outperforms biodiesel blends across all parameters due to its higher volatility and better combustion characteristics.

In this study, WSA is used for optimisation. The optimisation process consists of three stages: (i) performing the trials, (ii) developing models for regression, and (iii) executing the optimisation of WSA. The factor points are provided in Table 2.

The experimental process involves 20 trials, as outlined in Table 3, utilising the specified factor values. In the second phase, regression equations are formulated for uncoded factor levels. Coded models are essential for the optimisation phase, while the uncoded models (original models) are also constructed to illustrate the true mathematical relationships for the readers. Consequently, the data provided in Table 4 are applied in the second phase for model development.

Table 2. Engine specifications.

Narrative	Standard
Model	Kirloskar, 4- stroke
Cooling	Water
Bore × stroke	78 mm × 62 mm
Displacement	325 cm^3
No. of cylinders	Mono
CR	18.5
Maximum speed	2600 rpm
Maximum power	4.1 kw
Fuel IT	14 ±1° bTDC
Fuel IP	19.6 MPa

Table 3. Level of factors.

Features	Notation	Levels			
		L1	L2	L3	L4
Biodiesel blends (vol. %)	X_1	B10	B20	B30	B40
BMEP (bar)	X_2	1.35	2.7	4.05	5.04

Table 4. Experimental runs.

Run	Uncoded factors		Responses					
	Biodiesel blend (vol. %)	BMEP (bar)	BTE (%)	BSFC (g/kWh)	NO_x (g/kWh)	HC (g/kWh)`	CO (g/kWh)	Smoke (%)
1	0	1.35	18.75	441	0.13	0.04	0.8	8.12
2	10	1.35	18.9	446	0.12	0.05	0.82	7.95
3	20	1.35	19.12	450	0.11	0.07	0.78	7.92
4	30	1.35	19.26	452	0.1	0.08	0.76	6.5
5	40	1.35	19.55	454	0.07	0.06	0.74	5.5
6	0	2.7	26.35	322	0.19	0.04	0.9	19.21
7	10	2.7	26.56	329	0.18	0.05	0.8	18.45
8	20	2.7	26.75	332	0.17	0.09	0.6	15.1
9	30	2.7	26.9	338	0.165	0.11	0.5	9.94
10	40	2.7	27.1	345	0.155	0.145	0.4	6.2
11	0	4.05	32.1	276	0.19	0.06	2.9	55
12	10	4.05	32.36	284	0.185	0.1	2.7	45
13	20	4.05	32.42	288	0.18	0.14	2.5	34
14	30	4.05	33.1	292	0.179	0.17	2.3	20.12
15	40	4.05	33.69	297	0.175	0.19	2.1	9.45
16	0	5.04	34.1	245	0.19	0.1	5.7	75
17	10	5.04	34.48	249	0.18	0.15	5.5	70
18	20	5.04	34.59	251	0.17	0.175	5.1	60
19	30	5.04	34.78	257	0.16	0.225	4.3	55
20	40	5.04	34.89	259	0.159	0.271	3.5	45

Equation (2) illustrates the full quadratic model used for the regression analysis:

$$Y = \beta_0 + \beta_1 X_1 + \beta_2 X_2 + \beta_{11} X_1^2 + \beta_{22} X_2^2 + \beta_{12} X_1 X_2 + \varepsilon. \quad (2)$$

In this expression, Y signifies the outcome variable, X represents the features, β stands for the coefficients, and ε denotes the residual error term [14,15]. Following several preliminary efforts, the model is established using linear terms for Y and com-

plete quadratic models for *Y*. Regression analysis and review of the model are conducted using Minitab, a commonly used analytical tool. The models related to both base factor levels and base outcomes are presented in Table 5. Figure 5 illustrates the surface plots for the outcomes, providing a clear sight of the parameter spaces.

Table 5. Level of factors.

BTE, %	7.617 + 9.205 BMEP (bar) + 0.0125 Blend % − 0.7931 BMEP (bar) · BMEP (bar) + 0.000171 Blend % · Blend % + 0.00136 BMEP (bar) · Blend %
BSFC, g/kWh	580.7 - 121.40 BMEP (bar) + 0.494 Blend % + 11.001 BMEP (bar) · BMEP (bar) − 0.0020 Blend % · Blend % + 0.0052 BMEP (bar) · Blend %
NO_x, g/kWh	0.0390 + 0.08241 BMEP (bar) − 0.001336 Blend % − 0.010425 BMEP (bar) · BMEP (bar) − 0.000002 Blend % · Blend % + 0.000165 BMEP (bar) · Blend %
HC, g/kWh	0.0410 − 0.00871 BMEP (bar) + 0.000486 Blend % + 0.00346 BMEP (bar) · BMEP (bar) − 0.000013 Blend % · Blend % + 0.000816 BMEP (bar) · Blend %
CO, g/kWh	1.315 − 0.991 BMEP (bar) + 0.0308 Blend % + 0.3374 BMEP (bar) · BMEP (bar) − 0.000279 Blend % · Blend % − 0.01256 BMEP (bar) · Blend %
Smoke, %	7.29 − 2.50 BMEP (bar) + 0.279 Blend % + 2.977 BMEP (bar) · BMEP (bar) − 0.00358 Blend % · Blend % − 0.2121 BMEP (bar) · Blend %

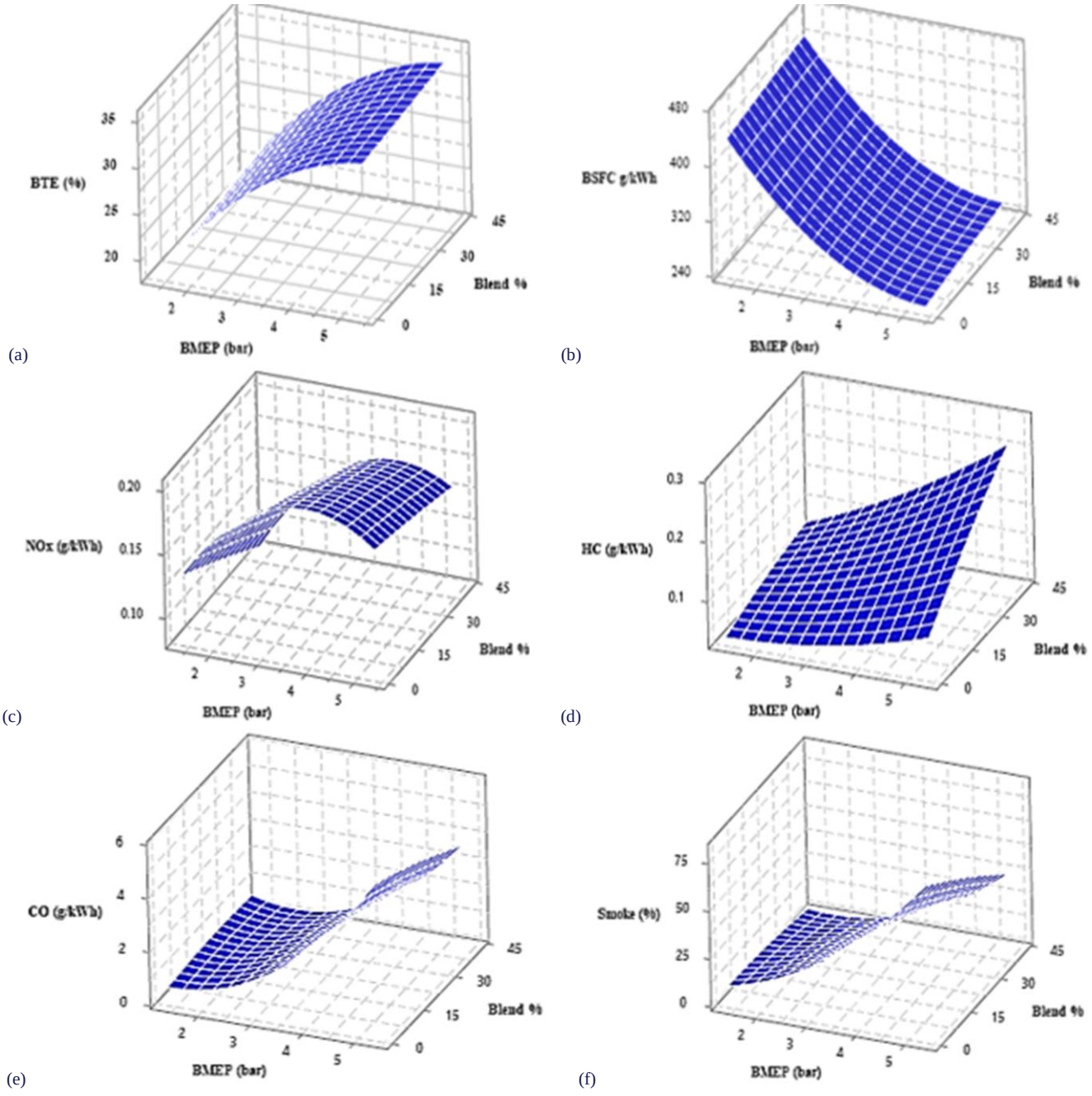

Fig. 5. Surface plots for responses (a) BTE, (b) BSFC, (c) NO_x, (d) HC, (e) CO (g/kWh) and (f) smoke opacity (%) vs. BMEP (bar).

The series of 3D surface plots provides a comprehensive analysis of the effects of BMEP and biodiesel blend percentage on various efficiency and exhaust features. BTE increases with BMEP, peaking at around 35% for moderate biodiesel blends (20–30%) at 5 bar, but remains below 25% at light loads (below 2 bar) due to inefficient combustion. Higher blends (above 40%) slightly reduce BTE due to lower calorific value, while D100 peaks at 33%, and JB30 achieves a maximum of 35%, showcasing the efficiency advantage of moderate blending. The brake specific fuel consumption (BSFC) decreases with increasing BMEP, dropping from 450 g/kWh at 1.5 bar to around 240 g/kWh at 5 bar, but increases with higher biodiesel blends due to lower calorific value, with JB40 showing 10–15% higher BSFC than D100 at all BMEP levels. NO_x emissions rise with both BMEP and blend percentage, peaking at 0.2 g/kWh for JB40 at 5 bar due to higher in-cylinder temperatures, while moderate blends like JB20 offer a balanced performance, producing 0.15–0.18 g/kWh at higher loads, and D100 shows the lowest NO_x emissions, particularly at light loads. Hydrocarbon (HC) emissions increase with BMEP, and are the lowest for the 0% blend, reaching around 0.05 g/kWh at 2 bar but rising with higher loads and blends. Carbon monoxide (CO) emissions also increase with BMEP, exceeding 6 g/kWh for higher blends at 5 bar, while remaining negligible at low BMEP for minimal blends. Similarly, smoke emissions intensify with rising BMEP and blend percentage, surpassing 50% at 4 bar and peaking near 75% for a 45% blend, emphasising the compounding impact of engine load and biodiesel blending on particulate formation and burning features.

Table 6 presents the R^2 values for these models. To be suitable for optimisation, the R^2 values should approach 1 (100%). In this case, it is concluded that the factors included in the model sufficiently explain the variation in the response.

Table 6. Computed values for the coefficient of determination.

Determination of coefficient	Outcomes					
	BTE (%)	BSFC (g/kWh)	NOx (g/kWh)	HC (g/kWh)	CO (g/kWh)	Smoke (%)
R^2 (%)	99.71	99.17	96.23	98.24	98.43	97.34
R^2 (%) predicted	99.41	98.49	89.48	95.53	96.29	93.37
R^2 (%) adjusted	99.61	98.87	94.88	97.61	97.87	96.39

Table 6 presents the computed coefficients of determination (R^2, adjusted R^2, and predicted R^2) obtained using Minitab. To ensure the models' validity, their significance must be evaluated. This is achieved through ANOVA (analysis of variance), a statistical method that uses the F-test to assess the consequence of regression models. As shown in Table 7, the p-values for all models are 0.000, confirming the statistical significance of the regression models. Table 8 provides the tuning factors of the WSA approach along with their description [15].

Table 7. Regression models for all responses.

	BTE (%)		BSFC (g/kWh)		F-value		p-value	
Cause	F-value		p-value					
Model	978.80		0.000		332.97		0.000	
Linear	2306.71		0.000		771.34		0.000	
BMEP (bar)	4597.96		0.000		1531.31		0.000	
Blend %	15.46		0.002		11.37		0.002	
Square	140.24		0.000		61.08		0.000	
BMEP (bar) × BMEP (bar)	280.37		0.000		122.13		0.000	
Blend (%) × Blend (%)	0.11		0.745		0.03		0.859	
2 way interaction	0.11		0.741		0.00		0.952	
BMEP (bar) × Blend %	0.11		0.741		0.00		0.952	

	NO_x (g/kWh)		HC(g/kWh)		CO(g/kWh)		Smoke (%)	
Cause	F-value	p- value	F- value	p- value	F- value	p- value	F- value	p- value
Model	71.43	0.000	156.10	0.000	175.99	0.000	102.39	0.000
Linear	115.49	0.000	356.37	0.000	73.61	0.000	231.41	0.000
BMEP (bar)	181.30	0.000	424.88	0.000	716.97	0.000	397.00	0.000
Blend %	49.68	0.002	287.87	0.002	30.25	0.000	65.82	0.000
Square	61.00	0.000	4.33	0.000	55.82	0.000	14.55	0.000
BMEP (bar) × BMEP (bar)	121.96	0.000	7.74	0.000	111.00	0.438	28.75	0.000
Blend (%) × Blend (%)	0.04	0.745	0.93	0.859	0.64	0.000	0.35	0.563
2 way interaction	4.20	0.741	59.07	0.952	21.10	0.000	20.02	0.001
BMEP (bar) × Blend %	4.20	0.741	59.07	0.952	21.10		20.02	0.001

Table 8. Control parameters of WSA algorithm.

Elements	Description	Standard
Maxtler	Max. iteration number	40,000
Ns	Solutions generated in each cycle	40
τ	Adjustable elements	0.7
Φ	Adjustable elements	0.0001
Λ	Adjustable elements	0.755
Sl₀	Primary step size	0.001

The WSA approach determined the tuned variable levels to be X_1 = 40 (unscaled variable level: 1) and X_2 = 1.648056 (unscaled variable level: 0.944899). However, since X_2 = 1.648056 is not practical, it has been adjusted to 1.6 (unscaled variable level: 0.96) by rounding to the nearest suitable value.

The given dataset in Table 9 represents optimal engine settings due to its balanced performance and emissions characteristics.

Table 9. Validation of response optimisation.

Blend (%)	BMEP (bar)	BTE %	BSFC g/kWh	NO_x g/kWh	HC g/kWh	CO g/kWh	Smoke (%)
40	2.74091	27.812	347.72	0.1480	0.1311	0.5448	4.9815

A BMEP of 2.74 bar reflects a moderate torque output, ensuring sufficient engine performance without overstressing components or increasing fuel consumption excessively. The brake thermal efficiency (BTE) of 27.81% indicates effective energy conversion, striking a good balance between the fuel efficiency and power output. While BSFC of 347.72 g/kWh suggests relatively high fuel consumption, it reflects a compromise necessary to maintain lower emissions and engine reliability. The low NO_x emissions (0.148 g/kWh) highlight effective control of combustion temperatures, reducing harmful pollutants to meet environmental standards. Similarly, moderate HC (0.1311 g/kWh) and CO (0.5448 g/kWh) levels demonstrate reasonably complete combustion while preserving engine efficiency. Finally, the low smoke percentage of 4.98% indicates minimal particulate emissions, ensuring compliance with air quality standards.

4. Conclusions

- Diesel (D100) achieves the ultimate BTE of 38% at 5.04 bar, with BSFC around 200 g/kWh, while biodiesel blends like JB10 and JB20 follow closely with BTE values of 37−38% and BSFC of 210–220 g/kWh. At a lower BMEP (1.35 bar), BTE for all fuels ranges between 15–17%, with biodiesel blends like JB40 showing the largest drop and higher BSFC (450–470 g/kWh).
- NO_x and HC emissions rise with BMEP and biodiesel content, with biodiesel blends (especially JB30 and JB40) showing higher NO_x emissions due to increased combustion temperatures.
- CO emissions and smoke opacity increase significantly at a higher BMEP, with JB40 peaking at 5.5 g/kWh for CO and 70% for smoke opacity, indicating incomplete combustion in higher biodiesel blends.
- The optimal engine settings with a balanced performance profile achieve a moderate torque (BMEP of 2.74 bar) and effective energy conversion (BTE of 27.81%).
- The relatively high BSFC (347.72 g/kWh) is balanced by low emissions of CO (0.5448 g/kWh), NO_x (0.148 g/kWh, and smoke opacity (4.98%), ensuring both efficiency and environmental compliance. These settings optimise engine performance while adhering to emissions standards.
- The WSA algorithm was applied to determine the optimal factor levels based on the regression models. Subsequent confirmation tests validated these optimised settings, showing that BTE was maximised while emissions and other response parameters were effectively minimised.

References

[1] Stančin, H., Mikulcic, H., Wang, X., & Duic, N. (2020). A review on alternative fuels in future energy system. *Renewable and Sustainable Energy Reviews*, 128:109927. doi: 10.1016/j.rser.2020.109927

[2] Zhang, Z., Wang, S., Pan, M., Lv, J., Lu, K., Ye, Y., & Tan, D. (2024). Utilization of hydrogen-diesel blends for the improvements of a dual-fuel engine based on the improved Taguchi methodology. *Energy*, 292, 130474. doi: 10.1016/j.energy.2024.130474

[3] Debella, H.A., Ancha, V.R., Atnaw, S.M., & Zeleke, D.S. (2024). Experimental study on performance and emissions from Prosopis juliflora biodiesel blends with diethyl ether additives. *Energy Conversion and Management: X*, 22, 100581. doi: 10.1016/j.ecmx.2024.100581

[4] Jaiganesh, J., Prakash, R., & Krishnan, M.G. (2024). Exploring the synergistic potential of prosopis juliflora and waste plastic oil biodiesel through investigation of performance, combustion, and emission in a CRDI engine: A shift towards Sustainable Fuel. *Process Safety and Environmental Protection*, 184, 720–735. doi: 10.1016/j.psep.2024.02.036

[5] Kukana, R., & Jakhar, O.P. (2021). Synthesis of biodiesel from Prosopis juliflora and using MCDM analytical hierarchy process

technique for evaluating with different biodiesel. *Cogent Engineering*, 8(1). doi: 10.1080/23311916.2021.1957291

[6] Sasikumar, R., Sankaranarayanan, G., & Karthikeyan, R. (2022). Investigation characteristics of Prosopis juliflora biodiesel blended with diesel fuel in a DI diesel engine. *Australian Journal of Mechanical Engineering*, 20(3), 692–697. doi: 10.1080/14484846.2020.1740021

[7] Kumar, S., Ningegowda, B.A., & Raju, V.D. (2022). The combined influence of injection pressure and exhaust gas recirculation on the characteristics of the diesel engine fuelled with Juliflora Biodiesel. *International Journal of Ambient Energy*, 43(1), 7952–7961. doi: 10.1080/01430750.2022.2075929

[8] Selvan, P.T., & Goteti, G.S. (2020). Experimental analysis of VCR engine operated with Prosopis juliflora biodiesel blends. *International Journal of Renewable Energy Research*, 10(2). doi: 10.20508/ijrer.v10i2.10776.g7965

[9] Abbas, A.M., Alomran, M.M. Alharbi, N.K. & Novak, S.J. (2023). Suppression of Seedling Survival and Recruitment of the Invasive Tree Prosopis juliflora in Saudi Arabia through Its Own Leaf Litter: Greenhouse and Field Assessments. *Plants*, 12(4). doi: 10.3390/plants12040959

[10] Vinodraj, S., Arularasan, R., Karthikeyan, D., Sethuraman, N., & Suryavarman, K. (2023). Impact of non-edible biodiesel (Juliflora oil seed) on CI engine – combustion, performance and emission features. *Materials Today: Proceedings*. doi: 10.1016/j.matpr.2023.05.306

[11] Musthafa, B., Saravanan, B., Vaibhav, B., Muhammad, P., Sam, F., & Asokan, M.A. (2023). Performance and emission analysis of a diesel engine fuelled with Juliflora Biodiesel: A simulation and experimental study. *Australian Journal of Mechanical Engineering*, 23(1), 220–234. Doi: 10.1080/14484846.2023.2274999

[12] Musthafa, B., & Asokan, M.A. (2024). Numerical and experimental investigation of performance and emission characteristics of hydrogen enrichment with prosopis juliflora biodiesel in CI engine using RSM and ANN optimization. *International Journal of Hydrogen Energy*, 66, 326–336. doi: 10.1016/j.ijhydene.2024.04.083

[13] Duraisamy, B., Velmurugan, K., & Venkatachalapathy, V.S. (2022). Analysis of prosopis juliflora methyl ester as a fuel in the CI engine. *International Journal of Research and Review*, 9(7), 112–118. doi: 10.52403/ijrr.20220713

[14] Mason, R.L., Gunst, R.F., & Hess, J.L. (2003).*Statistical design and analysis of experiments: with applications to engineering and science* (2nd ed.). John Wiley & Sons.

[15] Simsek, D., Ozyurek, D., Ileri, E., Akpinar, S., Karaoglan, A.D. (2022). Optimizing of Wear Performance on Elevated Temperature of ZrO_2 Reinforced AMCs Using Weighted Superposition Attraction Algorithm. *Journal of Scientific & Industrial Research*, 81, 462–474. doi: 10.56042/jsir.v81i05.47027

[16] Baykasoğlu, A., & Akpinar, S. (2015). Weighted Superposition Attraction (WSA): A swarm intelligence algorithm for optimization problems–Part 2: Constrained optimization. *Applied Soft Computing*, 37, 396–415. doi: 10.1016/j.asoc.2015.08.052